

# Polarization enhancement in two- and three-component ferroelectric superlattices

S. M. Nakhmanson, K. M. Rabe, and David Vanderbilt

Department of Physics and Astronomy, Rutgers University, Piscataway, NJ 08854-8019

(Dated: August 15, 2018)

Composition-dependent structural and polar properties of epitaxial short-period  $\text{CaTiO}_3/\text{SrTiO}_3/\text{BaTiO}_3$  superlattices grown on a  $\text{SrTiO}_3$  substrate are investigated with first-principles density-functional theory computational techniques. Polarization enhancement with respect to bulk tetragonal  $\text{BaTiO}_3$  is found for two- and three-component superlattices with a  $\text{BaTiO}_3$  concentration of more than 30%. Individual  $\text{BaTiO}_3$  layer thickness is identified as an important factor governing the polarization improvement. In addition, the degree of inversion-symmetry breaking in three-component superlattices can be controlled by varying the thicknesses of the component layers. The flexibility allowed within this large family of structures makes them highly suitable for various applications in modern nano-electro-mechanical devices.

With modern state-of-the-art epitaxial engineering techniques, complex perovskite oxide superlattices with three different constituent layers can be grown to realize a wide range of designer materials for a variety of applications.<sup>1,2,3</sup> Recently, it was shown that hundreds of atomically thin individual layers of  $\text{CaTiO}_3$  (CT),  $\text{SrTiO}_3$  (ST) and  $\text{BaTiO}_3$  (BT) could be grown on a perovskite ST substrate, yielding superlattices with compositionally abrupt interfaces, atomically smooth surfaces and excellent polar properties.<sup>2,3</sup> Since the relaxed lattice constants of CT and BT are 0.07 Å smaller and 0.11 Å larger than that of ST (3.905 Å), respectively, epitaxial strain in such structures results in substantial polarization enhancement.<sup>4</sup> In addition, the inversion symmetry breaking present in three-component superlattices<sup>2,3,5</sup> leads to even greater flexibility in fine-tuning the ferroelectric properties of these materials.

In this letter, in the spirit of Ref. [4], we investigate structural and polarization-related properties of two-component (or “bicolor”) and three-component (“tricolor”)  $(\text{ST})_l(\text{BT})_m(\text{CT})_n$  ferroelectric superlattices, where  $l, n = 0, 1, 2$  and  $m = 0, \dots, 4$ , epitaxially matched to a cubic ST substrate. We demonstrate that a number of such structures have enhanced spontaneous polarization with respect to bulk tetragonal BT. We also show that, in agreement with the findings of Ref. [4], all superlattice layers, including the naturally-paraelectric ST ones, are strongly polarized, resulting in a smooth polarization profile along the [001] (epitaxial growth) direction in the structure.

All the calculations presented here were performed under periodic boundary conditions equivalent to the presence of short-circuited top and bottom “electrode” layers. A plane-wave based DFT-LDA method<sup>6</sup> with ultrasoft pseudopotentials<sup>7</sup> was utilized for the ionic relaxation of the  $1 \times 1 \times (l + m + n)$  supercells. 30 Ry wavefunction and 270 Ry electronic density plane-wave cutoffs were used in all the calculations. During the relaxations, the in-plane lattice constant  $a$  of the tetragonal cell was constrained to the theoretical lattice constant of cubic ST (3.858 Å in this investigation) and the out-of-plane lattice constant  $c$  was allowed to vary. The symmetry in all the calculations was restricted to space group  $P4mm$  (point group  $C_{4v}$ ), i.e., the ions could move only in the [001] direction. The system was considered to be at equilibrium when the Hellman-Feynman forces on the ions were less than  $0.5 \times 10^{-3}$  Ry/bohr and the  $\sigma_{33}$  component of the

stress-tensor was smaller than 0.5 KBar. We used a  $6 \times 6 \times N$  Monkhorst-Pack (MP) mesh<sup>8</sup> for all the Brillouin-zone integrations, where  $N = 6/(l + m + n)$  for  $l + m + n \leq 3$ ,  $N = 2$  for  $l + m + n = 4$  and  $N = 1$  for  $l + m + n \geq 4$ . We employed the Berry-phase method of the modern polarization theory<sup>9</sup> to compute the total polarization of each superlattice. The  $6 \times 6 \times 2N$  MP mesh used in the polarization calculations produced well-converged results.

Calculated structural parameters for the bicolor and tricolor  $(\text{ST})_l(\text{BT})_m(\text{CT})_n$  superlattices grown on ST, as well as for strained bulk CT and BT and unstrained bulk tetragonal BT, are presented in Table I. We find that bulk BT, with a relaxed lattice constant 2% larger than that of cubic ST, expands by 5.5% in the [001] direction when pseudomorphically constrained to the ST substrate. Analogously, CT, with relaxed lattice constant 1.2% smaller than that of the substrate, contracts by about 1%. These results are in excellent agreement with calculations of Diéguez *et al.*<sup>10</sup> The  $c/a$  ratios for the bicolor and tricolor superlattices show similar trends corresponding to BT layers expanding and CT layers slightly contracting. The tricolors have two sets of tabulated values because the lack of inversion symmetry in these systems makes ferroelectric displacements along [001] and  $[00\bar{1}]$  inequivalent. It is worth pointing out that the  $c/a$  values in the tricolor systems are slightly different for the [001] and  $[00\bar{1}]$  displacements, reflecting the presence of a polarization-strain coupling in the films. The experimental values for  $c/a$  ratios,<sup>11</sup> shown in parentheses for some structures, are in excellent agreement with the results of our calculations, with the only minor exceptions being for  $(\text{BT})_1(\text{CT})_1$  and tetragonal BT. Experimental parameters for the latter were obtained for a thin-film sample grown under the same conditions as the superlattice samples. The most likely source of discrepancy between the theoretical and experimental parameters in both of these cases could be the structural defects present in the experimentally grown thin films.

Turning to the polar properties of the superlattices, in columns 3 and 4 of Table I we assemble spontaneous polarizations  $P_{[001]}^{\text{BP}}$ , computed with the Berry-phase method, as well as polarization enhancement factors with respect to bulk tetragonal BT  $|P|/P_{t\text{-BT}}$  for all the superlattices and bulk materials studied in this investigation. Starting at the top of the Table, we notice that our calculations provide a very high polarization for strained bulk CT. With the aforementioned sym-

TABLE I: Structural parameters and polarization in bulk CT and BT, and in  $(\text{ST})_l(\text{BT})_m(\text{CT})_n$  superlattices, pseudomorphically grown on ST (with in-plane lattice constant  $a = 3.858 \text{ \AA}$ ).  $P_{[001]}^{\text{BP}}$  was computed with the Berry-phase method.  $|P|/P_{t\text{-BT}}$  is the polarization enhancement factor with respect to the polarization in bulk tetragonal BT. Experimental values, included for comparison, are shown in parentheses where available. The positive direction of the  $[001]$  axis is from the ST to the neighboring CT layer.

System	$c/a$	$P_{[001]}^{\text{BP}} \text{ (C/m}^2\text{)}$	$ P /P_{t\text{-BT}}$
Strained bulk:			
CT	0.9897	0.434	
BT	1.0548	0.368	
Bicolors:			
$(\text{ST})_1(\text{CT})_1$	1.976 (1.97)	0.026 (0.000)	0.11 (0.0)
$(\text{ST})_1(\text{BT})_1$	2.042 (2.07)	0.231 (0.059)	0.95 (0.54)
$(\text{BT})_1(\text{CT})_1$	2.019 (2.08)	0.231 (0.085)	0.95 (0.78)
$(\text{ST})_2(\text{CT})_2$	3.960	0.168	0.69
$(\text{ST})_2(\text{BT})_2$	4.088	0.245	1.01
$(\text{BT})_2(\text{CT})_2$	4.059	0.306	1.26
Tricolors:			
$(\text{ST})_1(\text{BT})_1(\text{CT})_1$	3.018	-0.200	0.82
	(3.02)	(0.030)	(0.28)
$(\text{ST})_2(\text{BT})_2(\text{CT})_2$	6.049	-0.239	0.98
	(6.05)	(0.069)	(0.63)
$(\text{ST})_2(\text{BT})_4(\text{CT})_2$	8.163	-0.295	1.21
	(8.21)	(0.133)	(1.22)
$(\text{ST})_3(\text{BT})_3(\text{CT})_3$	9.083	-0.260	1.07
	9.077	0.244	1.00
Bulk tetragonal BT	1.009 (1.026)	0.243 (0.109)	

metry restrictions in place, this is the polarization CT *would have* if the zone boundary distortions that are present in its actual ground-state crystal structure were suppressed. The DFT-based model of Diéguez *et al*<sup>10</sup> produces a similar result for the strained CT. However, this peculiar property does not automatically translate into highly polar CT-containing superlattices. While CT and BT are both ferroelectric in the (constrained) bulk, they behave quite differently in the superlattice geometries. BT is highly polar in monoatomic layer systems like  $(\text{ST})_1(\text{BT})_1$  or  $(\text{ST})_1(\text{BT})_1(\text{CT})_1$ , and becomes even more polar with growing BT-layer thickness  $m$ . This can be seen from the data for the “constant-concentration”  $(\text{ST})_m(\text{BT})_m$  and  $(\text{BT})_m(\text{CT})_m$  bicolor systems, and substantiated by the  $(\text{ST})_m(\text{BT})_m(\text{CT})_m$  tricolor series as well as the BT-rich  $(\text{ST})_2(\text{BT})_4(\text{CT})_2$  system. CT, at variance, is practically paraelectric in the monoatomic layer systems, with  $(\text{ST})_1(\text{CT})_1$  exhibiting low polarization and  $(\text{BT})_1(\text{CT})_1$  showing the same polarization as  $(\text{ST})_1(\text{BT})_1$ . However, as the thickness of the CT layer ( $n$ ) increases, so does its polarization: the  $(\text{ST})_2(\text{CT})_2$  system is substantially more polar than  $(\text{ST})_1(\text{CT})_1$ , and  $(\text{BT})_2(\text{CT})_2$  is more polar than  $(\text{ST})_2(\text{BT})_2$ . In  $(\text{ST})_3(\text{BT})_3(\text{CT})_3$ , the ferroelectric displacements in the CT layer are larger than those in the BT layer. These results suggest that CT and BT cells tend to remain

more polar when assembled into thick layers, as opposed to being intermixed with each other and naturally paraelectric ST.<sup>12</sup> However, in experimentally studied systems, epitaxial growth restrictions place a limit on the values of  $n$  and  $m$ .<sup>13</sup> Above a certain thickness, CT or BT layers relax to their native in-plane lattice constants and the strain-induced polarization enhancement is lost. For example, in the  $(\text{ST})_2(\text{BT})_m(\text{CT})_2$  superlattices, the polarization starts to decrease at  $m \simeq 7$ ,<sup>3,11</sup> so that a delicate balance between concentration and layer thickness has to be maintained to produce superlattices with the strongest polarization enhancement. Finally, there is an additional degree of tunability of polar properties in the tricolor superlattice family. As shown in the bottom part of the Table, the inequivalence of the  $[001]$  and  $[00\bar{1}]$  ferroelectric displacement directions results in two distinct values of polarization in these structures.

Experimental values for the spontaneous polarizations in some ferroelectric superlattices, obtained by Lee *et al*,<sup>3,11</sup> together with the associated polarization enhancement factors are shown for comparison in Table I. The former are consistently smaller than the polarizations obtained in the calculations. However, during the experimental sequences of poling and polarization reversal, structural defects and incomplete switching of ferroelectric domains usually do lead to substantially reduced values of remanent polarization. Our calculations, on the other hand, correspond to an “ideal case” (no defects and perfect switching) and thus provide upper-bound polarization estimates. Nevertheless, if we compare enhancement factors instead of actual polarizations, we see certain similar trends in the experimental and theoretical data. For example, experimental results for the tricolor systems show the same sequence of polarization enhancement (from  $(\text{ST})_1(\text{BT})_1(\text{CT})_1$  to  $(\text{ST})_2(\text{BT})_4(\text{CT})_2$ ) as the calculated one. Also the agreement between theoretical and experimental polarization-enhancement factors in tricolor systems improves with increasing polarization of the system. The predicted difference in polarizations induced by inequivalent ionic displacements in the tricolor superlattices has not yet been observed in the samples of Lee *et al* due to other sources of asymmetry in the experimental geometries.<sup>3,11</sup>

Since the intricate relation between pseudomorphic strain and chemical composition of the layers is the key to the polarization enhancement in the superlattices, we investigated the layer-by-layer polarization behavior in these structures. Density-functional perturbation theory<sup>14</sup> was used to obtain Born effective charges for ions in relaxed supercells, and these were then used to decompose an “aggregate” supercell polarization into contributions from individual primitive cells comprising each superlattice. The polarization contribution  $P_\lambda$  from cell  $\lambda$  was estimated using the linearized approximation

$$P_\lambda \simeq \sum_i \frac{\partial P}{\partial u_{\lambda i}^{(0)}} (u_{\lambda i} - u_{\lambda i}^{(0)}) = \frac{1}{V_\lambda} \sum_i Z_{\lambda i}^* \Delta u_{\lambda i}, \quad (1)$$

where  $Z_{\lambda i}^*$  and  $\Delta u_{\lambda i}$  are the effective charge and displacement of ion  $i$  in cell  $\lambda$ , and  $V_\lambda$  is the volume of the cell. All polarizations and ionic displacements are constrained to the  $[001]$  direction, and a superscript zero refers to a non-polar structure with ferroelectric displacement removed by “unbuckling” the

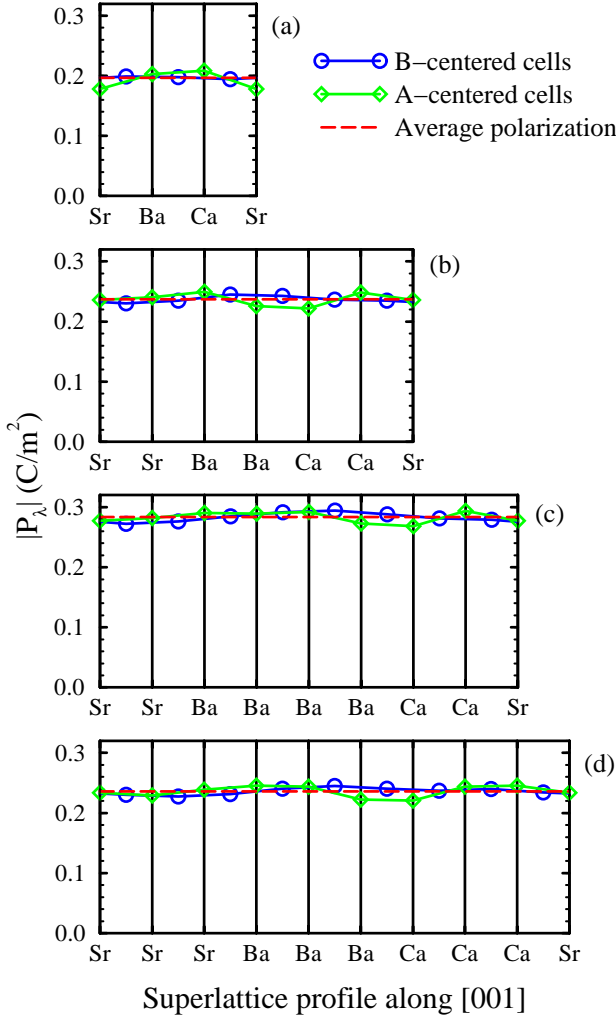


FIG. 1: Examples of local polarization profiles of the tricolor  $(ST)_l(BT)_m(CT)_n$  superlattices: (a)  $l, m, n = 1$ ; (b)  $l, m, n = 2$ ; (c)  $l, n = 2, m = 4$ ; (d)  $l, m, n = 3$ . Dashed lines show the absolute value of total average polarization in the supercells ( $P_{[001]}^{BEC}$ ).

AO and BO planes and moving the “middle” planes back to the center of each primitive cell. Equation (1) can be used with either A or B cation-centered cells. In each case we average out contributions of the oxygens in the planes bounding

elementary cells, while cations at the corners set the volume of each cell. The total supercell polarization  $P_{[001]}^{BEC}$  can be recovered from Eq. (1) by extending the summation to all the ions in the system. Total polarizations obtained by such summations are in good agreement with those computed by the Berry-phase method.

In Fig. 1 we present the layer-by-layer polarization profiles of the tricolor superlattices from Table I. Both A and B cation-centered cell profiles are shown for each superlattice, but the differences between the two are small. Both types of analysis show that all of the layers in the superlattice structures (including the naturally paraelectric ST ones) are strongly polarized, and that the local polarization is almost uniform throughout the superlattice. As already pointed out in Ref. [4], the near constancy of polarization throughout the superlattice results from the minimization of the energy terms associated with the polarization charge build-up ( $\nabla \cdot \mathbf{P}$ ) at the interfaces (i.e., it is energetically unfavorable for the system to have a large divergence of the polarization).

In summary, we have used first-principles methods to study structural properties and polarization enhancement in short-period perovskite-type thin films containing individual layers of CT, ST and BT. We find that the presence of highly polar CT and BT layers induces substantial polarization in these superlattices. The actual degree of polarization enhancement strongly depends on an interplay between the concentration of ferroelectric components in the superlattice and the pseudomorphic strain it can sustain. Maximum polarization enhancement is achieved by the highest concentration of CT or BT assembled into the thickest possible layers that are still consistent with a state of full epitaxial strain. Our calculations also show that the tricolor superlattices that lack a center of inversion have two distinct values of polarization depending on the direction of the ferroelectric displacement, which can be exploited for fine-tuning of the polar properties. We hope that this investigation, by providing additional insight into the nature of complex polar perovskite materials, will lead to better understanding and control of their properties in the quest for more efficient and environmentally friendly nano-electro-mechanical devices.

The authors thank H. N. Lee for sharing his data and many valuable discussions. This work was supported by the Center for Piezoelectrics by Design (CPD) under ONR Grant N00014-01-1-0365.

- <sup>1</sup> H. Yamada, M. Kawasaki, Y. Ogawa, and Y. Tokura, Appl. Phys. Lett. **81**, 4793 (2002).
- <sup>2</sup> M. P. Warusawithana, E. V. Colla, J.N. Eckstein, and M. B. Weissman, Phys. Rev. Lett. **90**, 036802 (2003).
- <sup>3</sup> H. N. Lee, H. M. Christen, M. F. Chisholm, C. M. Rouleau and D. H. Lowndes, Nature **433**, 395 (2005).
- <sup>4</sup> J. B. Neaton and K. M. Rabe, Appl. Phys. Lett. **82**, 1586 (2003).
- <sup>5</sup> N. Sai, B. Meyer and D. Vanderbilt, Phys. Rev. Lett. **84**, 5636 (2000).
- <sup>6</sup> We used PWscf code (available from <http://www.pwscf.org>) for

- the calculations presented here.
- <sup>7</sup> D. Vanderbilt, Phys. Rev. B **41**, 7892 (1990).
- <sup>8</sup> H. J. Monkhorst and J. D. Pack, Phys. Rev. B **13**, 5188 (1976).
- <sup>9</sup> R. D. King-Smith and D. Vanderbilt, Phys. Rev. B **47**, 1651 (1993); R. Resta, Rev. Mod. Phys. **66**, 899 (1994).
- <sup>10</sup> O. Diéguez, K. M. Rabe and D. Vanderbilt, to be published.
- <sup>11</sup> H. N. Lee, private communication.
- <sup>12</sup> This is conceptually very similar to polarization behavior in polymer ferroelectrics. See S. M. Nakhmanson, M. Buongiorno-Nardelli and J. Bernholc, to be published.

- <sup>13</sup> K. J. Choi, M. Biegalski, Y. L. Li, A. Sharan, J. Schubert, R. Uecker, P. Reiche, Y. B. Chen, X. Q. Pan, V. Gopalan, L.-Q. Chen, D. G. Schlom, C. B. Eom, *Science* **306**, 1005 (2004);
- <sup>14</sup> S. Baroni, S. de Gironcoli, A. Dal Corso and P. Giannozzi, *Rev. Mod. Phys.* **73**, 515 (2001).